ELSEVIER

Journal of Chromatography A, 734 (1996) 105–123

JOURNAL OF CHROMATOGRAPHY A

Multi-component perfusion chromatography in fixed bed and periodic counter current column operation

G.A. Heeter, A.I. Liapis*

Department of Chemical Engineering and Biochemical Processing Institute, University of Missouri-Rolla, Rolla, MO 65401-0249, USA

Abstract

A mathematical model of multi-component dynamic adsorption in columns with spherical perfusive and spherical purely diffusive adsorbent particles with a bidisperse porous structure is constructed, solved, and used to study the performance of a binary adsorption system in a single-column fixed-bed process and in a two-column periodic counter-current process in which the adsorbent is equally distributed over two beds. The total length of the two-column periodic counter-current system is equal to the length of the single-column fixed-bed system. The performance of fixed-bed and periodic counter-current systems with both perfusive and purely diffusive adsorbent particles is examined for different values of the macropore void fraction, ϵ_p, the particle diameter, d_p, the inlet concentration of the least preferentially adsorbed component 2, $C_{d2,in}$, and the superficial velocity, V_f. For the binary adsorption system studied in this work, the results show that the adsorption column must be operated in the periodic counter-current mode at low values of the superficial velocity, V_f, in order to achieve high relative separation efficiency. Under these conditions, the performance of the adsorption column does not depend upon ϵ_p or d_p. The relative separation efficiency decreases somewhat and is no longer independent of ϵ_p and d_p when V_f is increased moderately. At high values of V_f, the relative separation efficiency is unsatisfactory for all cases. The performance of systems with perfusive adsorbent particles is slightly better than the performance of systems with purely diffusive adsorbent particles for some values of V_f.

Keywords: Perfusion chromatography; Periodic counter-current system; Adsorption; Multi-component adsorption; Mathematical models

1. Introduction

In this work, as in previous publications [1–8], we define "perfusion chromatography" to refer to any chromatographic system in which the intraparticle velocity, v_p, is non-zero [1–10].

Liapis and McCoy [4], Liapis et al. [5], Heeter and Liapis [7], and Xu and Liapis [8] have considered that the perfusive adsorbent particles with a bidisperse [4,5,7,8] porous structure have a macroporous region made by the through-pores (macropores) [1,3–5,7–9] in which intraparticle convection and pore diffusion occur, and a microporous [4,5,7,8] region made by spherical microparticles (microspheres [4,5,7,8]) that are taken to be purely diffusive. Liapis et al. [5] and Xu and Liapis [8] studied the performance of the adsorption and elution stages of single-component adsorption in columns packed with spherical perfusive and spherical purely diffusive adsorbent particles with a bidisperse porous structure. Heeter and Liapis [7] studied the performance of the adsorption stage of systems involving single-component adsorption of bovine serum albumin (BSA) into spherical bidisperse perfusive and spheri-

*Corresponding author.

0021-9673/96/$15.00
SSDI 0021-9673(95)01147-1

cal bidisperse purely diffusive anion exchange porous adsorbent particles in a single-column fixed-bed system and in a two-column periodic counter-current system in which the adsorbent is equally distributed over two beds; the total length of the two-column periodic counter-current system was equal to the length of the single-column fixed-bed system.

McCoy et al. [2] examined the performance of the adsorption stage of a single-column fixed-bed system involving the adsorption of a binary system (competitive adsorption involving two components) in perfusive and purely diffusive porous adsorbent particles of slab geometry. In this work, a mathematical model for the adsorption stage of multicomponent adsorption in columns packed with spherical perfusive and spherical purely diffusive adsorbent particles with a bidisperse porous structure is presented, and used to study the performance of a binary adsorption system in a single-column fixed-bed process and in a two-column periodic counter-current process in which the adsorbent is equally distributed over two beds; the total length of the two-column periodic counter-current system is taken to be equal to the length of the single-column fixed-bed system.

2. Mathematical Model

Adsorption is considered to take place from a flowing liquid stream in a single-column fixed-bed system of spherical perfusive adsorbent particles having a bidisperse porous structure [1,4,5,7–9], under isothermal conditions. The concentration gradients in the radial direction of the bed are considered to be not significant [11–13]. The feed solution to the bed is considered to contain n components, and m ($m < n$) solutes may compete for the available active sites for specific adsorption; also, $m+1 \le i \le l$ ($l < n$) solutes may be non-specifically adsorbed, and $l+1 \le i \le n$ solutes are simply transported by intraparticle convection and diffusion into the pores of the particles without interacting with the adsorbent [11,14]. A differential mass balance for each component in the flowing fluid stream gives

$$\frac{\partial C_{di}}{\partial t} - D_{Li}\frac{\partial^2 C_{di}}{\partial x^2} + \frac{V_f}{\epsilon}\frac{\partial C_{di}}{\partial x} = -\frac{(1-\epsilon)}{\epsilon}\frac{\partial \bar{C}_{psi}}{\partial t}, \quad i = 1,2,\ldots,n. \tag{1}$$

In Eq. 1, the superficial velocity of the fluid stream, V_f, is taken to be independent of the space variable x, because the liquid solutions encountered in many chromatographic systems are most often very dilute and the main component of the solution is the carrier fluid. For non-dilute solutions, a material balance, as shown by Harwell et al. [15], would provide the expression for $\partial V_f / \partial x$. The pressure drop through the fixed-bed, which is important in the design of an adsorption fixed-bed system, can be determined by the methods reported in Refs. [16] and [17]. The initial and boundary conditions of Eq. 1 are as follows:

$$C_{di} = 0 \text{ at } t = 0, 0 \le x \le L, i = 1,2,\ldots,n, \tag{2}$$

$$\frac{V_f}{\epsilon}C_{di} - D_{Li}\frac{\partial C_{di}}{\partial x} = \frac{V_f}{\epsilon}C_{di,in} \quad \text{at } x = 0, t > 0, i = 1,2,\ldots,n, \tag{3}$$

$$\frac{\partial C_{di}}{\partial x} = 0 \quad \text{at } x = L, t > 0, i = 1,2,\ldots,n. \tag{4}$$

The value of $C_{di,in}$ may be constant or it may vary with time. Expressions for estimating D_{Li} were presented by Arnold et al. [18] and Gunn [19,20], but in certain systems the axial dispersion is so low that by setting its value equal to zero, the error introduced in the prediction of the behavior of an affinity adsorption system is not significant [13,18]. When the axial dispersion coefficient is set equal to zero, Eqs. 1 and 3 (with $D_{Li} = 0$) become

$$\frac{\partial C_{di}}{\partial t} + \frac{V_f}{\epsilon}\frac{\partial C_{di}}{\partial x} = -\frac{(1-\epsilon)}{\epsilon}\frac{\partial \bar{C}_{psi}}{\partial t}, \quad i = 1,2,\ldots,n, \tag{1a}$$

$$C_{di} = C_{di,in} \quad \text{at } x = 0, t > 0, i = 1,2,\ldots,n. \tag{3a}$$

The spherical perfusive adsorbent particles with a bidisperse [4,5,7,8] porous structure are considered to have a microporous [4,5,7,8] region made by spherical microparticles (microspheres [4,5,7–9]) that are taken to be purely diffusive, and a macroporous [4,5,7,8] region made by the through-pores [1,3–5,7–9] in which intraparticle convection and pore diffusion occur. In Fig. 1 of Ref. [5], a diagram of a spherical perfusive adsorbent particle with a bidisperse porous structure is presented; the coordinate system of the spherical perfusive adsorbent

particle shown in Fig. 1 of Ref. [5] is also used in this work, and x_1 again represents the axial coordinate for the spherical perfusive adsorbent particle and is parallel to the axial coordinate x of the column. The adsorption process is considered to be isothermal, as the heats of adsorption apparently do not change the temperature [1,12] of the liquid phase even in large-scale systems; this occurs because the total amount of adsorbed material is small and the heat capacity of the liquid phase is high.

The differential mass balance for each component i in the macroporous region of a perfusive adsorbent particle of spherical geometry is given by

$$\epsilon_p \frac{\partial C_{pi}}{\partial t} + \epsilon_p v_{pR} \frac{\partial C_{pi}}{\partial R} + \epsilon_p v_{p\theta} \left(\frac{1}{R}\right) \frac{\partial C_{pi}}{\partial \theta} + (1-\epsilon_p) \frac{\partial \bar{C}_{si}}{\partial t}$$
$$= \epsilon_p \left[\left(\frac{1}{R^2}\right) \left(\sum_{j=1}^{n} \frac{\partial}{\partial R} \left(R^2 D_{pij} \frac{\partial C_{pj}}{\partial R} \right) \right) + \left(\frac{1}{R^2 \sin\theta} \right) \left(\sum_{j=1}^{n} \frac{\partial}{\partial \theta} \left(\sin\theta \, D_{pij} \frac{\partial C_{pj}}{\partial \theta} \right) \right) \right],$$
$$i = 1,2,\ldots,n. \tag{5}$$

In Eq. 5, surface diffusion [1,12] of the adsorbed species on the surface of the macropores is not considered, because the contribution of the surface diffusion mass flux to the overall mass flux is taken to be negligible relative to the contributions of the pore diffusion mass flux and of the intraparticle convection; the contribution of the surface diffusion mass flux is considered to be negligible because (i) the surface area of the macroporous region is often significantly smaller than the surface area of the microporous region (most of the adsorptive capacity of the perfusive adsorbent particle is in the microporous region), and (ii) in many systems involving mixtures of biological macromolecules the interaction between the adsorbate(s) and the active sites on the surface of the macropores could be strong [1,12], and therefore surface diffusion could be insignificant. The variables v_{pR} and $v_{p\theta}$ represent the intraparticle velocity components along the R and θ directions, respectively. The expressions for v_{pR} and $v_{p\theta}$ are given in Eqs. 7 and 8 of Ref. [5]. For the multicomponent system studied in this work, the value of the parameter H in Eqs. 7 and 8 of Ref. [5] is essentially equal to zero. When the value of H is set equal to zero in Eqs. 7 and 8 of Ref. [5], the following expressions for v_{pR}, $v_{p\theta}$, and v_{px_1} (v_{px_1} is the axial component of the intraparticle velocity which is parallel to the flowing fluid stream along the axis of the column, and its expression is given in Eq. 18 of Ref. [5]) are obtained:

$$v_{pR} \cong F V_f \cos\theta, \tag{6}$$

$$v_{p\theta} \cong -F V_f \sin\theta, \tag{7}$$

$$v_{px_1} = F V_f. \tag{8}$$

The mixtures of components to be separated by chromatographic systems are usually dilute (this is most often the case for mixtures of biological macromolecules), especially with respect to the component(s) of interest, and therefore it may be possible to set the off-diagonal (D_{pij}, $i \neq j$) elements of the effective pore diffusivity matrix, $\mathbf{D}_p$, equal to zero [1,12,21,22]. In this case, Eq. 5 would take the following form:

$$\epsilon_p \frac{\partial C_{pi}}{\partial t} + \epsilon_p v_{pR} \frac{\partial C_{pi}}{\partial R} + \epsilon_p v_{p\theta} \left(\frac{1}{R}\right) \frac{\partial C_{pi}}{\partial \theta} + (1-\epsilon_p) \frac{\partial \bar{C}_{si}}{\partial t}$$
$$= \epsilon_p D_{pii} \left[\left(\frac{1}{R^2}\right) \frac{\partial}{\partial R} \left(R^2 \frac{\partial C_{pi}}{\partial R} \right) + \left(\frac{1}{R^2 \sin\theta} \right) \frac{\partial}{\partial \theta} \left(\sin\theta \frac{\partial C_{pi}}{\partial \theta} \right) \right],$$
$$i = 1,2,\ldots,n. \tag{5a}$$

In Eq. 5a, D_{pii} represent the diagonal terms (D_{pij}, $i=j$) of the effective pore diffusivity matrix, $\mathbf{D}_p$. Also, in Eqs. 5 and 5a, the term $\partial \bar{C}_{si}/\partial t$ becomes equal to zero for species that do not bind by specific or non-specific adsorption.

If the intraparticle Péclet number of component i, $\mathrm{Pe}_{\mathrm{intra},i}$, is defined by the expression

$$\mathrm{Pe}_{\mathrm{intra},i} = \frac{v_{px_1} d_p}{D_{pii}}, \quad i = 1,2,\ldots,n, \tag{9}$$

then, by using the expression for v_{px_1} given in Eq. 8, the following expression for $\mathrm{Pe}_{\mathrm{intra},i}$ is obtained:

$$\mathrm{Pe}_{\mathrm{intra},i} = \frac{v_{px_1} d_p}{D_{pii}} = \frac{(F V_f) d_p}{D_{pii}}, \quad i = 1,2,\ldots,n. \tag{10}$$

For purely diffusive adsorbent particles, $Pe_{intra,i}=0$ for $i = 1,2,\ldots,n$, while for adsorbent particles with non-zero intraparticle fluid flow, $Pe_{intra,i}>0$ for $i = 1,2,\ldots,n$.

The initial and boundary conditions of Eqs. 5 and 5a are as follows:

$$\text{at } t = 0, \quad C_{pi} = 0, \quad 0 \le R \le R_p, \quad i = 1,2,\ldots,n, \tag{11}$$

$$\text{at } R = R_p, \quad C_{pi} = C_{di}, \quad t > 0, \quad i = 1,2,\ldots,n, \tag{12}$$

$$\text{at } R = 0, \quad C_{pi} = \text{finite}, \quad t > 0, \quad i = 1,2,\ldots,n, \tag{13}$$

$$\text{at } \theta = 0, \quad \left.\frac{\partial C_{pi}}{\partial \theta}\right|_{\theta=0} = 0, \quad 0 \le R \le R_p, \quad i = 1,2,\ldots,n, \tag{14}$$

$$\text{at } \theta = \pi, \quad \left.\frac{\partial C_{pi}}{\partial \theta}\right|_{\theta=\pi} = 0, \quad 0 \le R \le R_p, \quad i = 1,2,\ldots,n. \tag{15}$$

Eq. 12 was obtained from the assumption that the external mass transfer resistance (the mass transfer resistance in a liquid film that may be located on the external particle surface) is not significant. Detailed calculations [11,23,24] have shown that the intraparticle mass transfer resistance is significantly larger than the external mass transfer resistance; for this reason, the external mass transfer resistance is taken to be negligible.

The differential mass balance for each component i in a purely diffusive spherical microparticle (microsphere) is given by

$$\epsilon_{pm}\frac{\partial C_{pmi}}{\partial t} + \left(\frac{1}{1-\epsilon_p}\right)\frac{\partial C_{smi}}{\partial t} = \frac{1}{r^2}\left[\epsilon_{pm}\left(\sum_{j=1}^{n}\frac{\partial}{\partial r}\left(r^2 D_{pmij}\frac{\partial C_{pmj}}{\partial r}\right)\right) + \left(\frac{1}{1-\epsilon_p}\right)\left(\sum_{j=1}^{n}\frac{\partial}{\partial r}\left(r^2 D_{smij}\frac{\partial C_{smj}}{\partial r}\right)\right)\right], \quad i = 1,2,\ldots,n. \tag{16}$$

The mixtures of components to be separated by chromatographic systems are usually dilute, and therefore it may be possible to set the off-diagonal (D_{pmij}, $i \neq j$; D_{smij}, $i \neq j$) elements of the effective pore diffusivity matrix, $\mathbf{D}_{pm}$, and of the surface diffusivity matrix, $\mathbf{D}_{sm}$, equal to zero [1,12,21,22]. If the interaction between the adsorbate(s) and the active sites on the surface of the pores is strong [1,12], then the surface diffusion may, in certain systems, be neglected. If the contribution of surface diffusion to mass transfer is insignificant and if the mixtures of the components to be separated are dilute, then Eq. 16 would become

$$\epsilon_{pm}\frac{\partial C_{pmi}}{\partial t} + \left(\frac{1}{1-\epsilon_p}\right)\frac{\partial C_{smi}}{\partial t} = \epsilon_{pm} D_{pmii}\left[\frac{\partial^2 C_{pmi}}{\partial r^2} + \frac{2}{r}\frac{\partial C_{pmi}}{\partial r}\right], \quad i = 1,2,\ldots,n. \tag{16a}$$

In Eq. 16a, D_{pmii} represent the diagonal terms (D_{pmij}, $i = j$) of the effective pore diffusivity matrix, $\mathbf{D}_{pm}$. Also, in Eqs. 16 and 16a the terms $\partial C_{smi}/\partial t$ and $\partial C_{smj}/\partial r$ become equal to zero for species which do not bind by specific or non-specific adsorption.

It is clear that Eq. 16a cannot be solved if an appropriate expression for the term $\partial C_{smi}/\partial t$ is not available. This term represents the accumulation of the adsorbed species i on the surface of the pores of the microsphere, and it can be quantified if a thermodynamically consistent mathematical model could be constructed that could describe the mechanism of adsorption for component i. For isothermal adsorption systems, the term $\partial C_{smi}/\partial t$ could be of the form

$$\frac{\partial C_{smi}}{\partial t} = f_i(\mathbf{C}_{pm}, \mathbf{C}_{sm}, \mathbf{k}), \quad i = 1,2,\ldots,m,m+1,\ldots,l \tag{17}$$

where f_i represents the functional form of the dynamic adsorption mechanism for component i; $\mathbf{C}_{pm}$ represents the concentration vector of the adsorbates in the pore fluid, $\mathbf{C}_{pm} = (C_{pm1}, C_{pm2}, \ldots, C_{pmm}, C_{pmm+1}, \ldots, C_{pml})$; $\mathbf{C}_{sm}$ denotes the concentration vector of the adsorbates in the adsorbed phase, $\mathbf{C}_{sm} = (C_{sm1}, C_{sm2}, \ldots, C_{smm}, C_{smm+1}, \ldots, C_{sml})$; and $\mathbf{k}$

represents the vector of the rate constants that characterize the interaction kinetics between the adsorbates and the active sites. For certain multicomponent adsorption systems, dynamic adsorption models of the form given in Eq. 17 have been constructed and presented in the literature [12,14,25–27].

In some adsorption systems, the rates of interaction between the adsorbates and the active sites may be much higher than the intraparticle convection and diffusional rates, and in such systems it may be possible to assume that equilibrium exists between the adsorbates in the pore fluid and in the adsorbed phase at each point in the pores. The term $\partial C_{smi}/\partial t$ in Eq. 16a, for systems where adsorption equilibrium may be assumed between the adsorbates in the pore fluid and in the adsorbed phase at each point in the pores, is then given by

$$\frac{\partial C_{smi}}{\partial t} = \sum_{j=1}^{l} \left(\frac{\partial g_i}{\partial C_{pmj}} \right) \left(\frac{\partial C_{pmj}}{\partial t} \right), \quad i = 1,2,\ldots,m,m+1,\ldots,l, \tag{18}$$

where

$$C_{smi} = g_i(\mathbf{C}_{pm},\mathbf{K}), \quad i = 1,2,\ldots,m,m+1,\ldots,l. \tag{19}$$

The functions g_i represent the equilibrium adsorption isotherms [23,25] for the adsorbates that may compete for the available (accessible) active sites on the surface of the pores. **K** represents the vector of the equilibrium constants that characterize the equilibrium interactions between the adsorbates and the active sites.

The initial and boundary conditions for Eq. 16a and the initial condition for Eq. 17 are as follows:

$$\text{at } t = 0, \quad C_{pmi} = 0 \quad \text{for} \quad 0 \le r \le r_m, \quad i = 1,2,\ldots,n, \tag{20}$$

$$\text{at } t = 0, \quad C_{smi} = 0 \quad \text{for} \quad 0 \le r \le r_m, \quad i = 1,2,\ldots,m,m+1,\ldots,l, \tag{21}$$

$$\text{at } r = r_m, \quad C_{pmi} = C_{pi}(t,R,\theta), \quad t > 0, \quad i = 1,2,\ldots,n, \tag{22}$$

$$\text{at } r = 0, \quad \left.\frac{\partial C_{pmi}}{\partial r}\right|_{r=0} = 0, \quad t > 0, \quad i = 1,2,\ldots,n. \tag{23}$$

At this point, it should be mentioned that the effective pore diffusivities D_{pii} and D_{pmii} in Eqs. 5a and 16a, respectively, could be determined by using a network model approach for bidisperse porous adsorbents, as indicated in Ref. [28]. Furthermore, the phenomena of restricted pore diffusion and percolation threshold could be treated by the theoretical approach presented in Ref. [29]. The network model theories presented in Refs. [28] and [29] require the pore-size distributions of the macroporous and microporous regions of the bidisperse porous adsorbent particle, the pore connectivities of the macropores and micropores, as well as the sizes of the molecules of the adsorbates and of the active sites.

The accumulation term $\partial \bar{C}_{si}/\partial t$ in Eqs. 5 and 5a is given [5,7] by the expression

$$\frac{\partial \bar{C}_{si}}{\partial t} = \frac{3}{r_m^3}\left[\frac{\partial}{\partial t}\left(\int_0^{r_m} \epsilon_{pm} C_{pmi} r^2 \, dr \right) + \frac{\partial}{\partial t}\left(\int_0^{r_m} \left(\frac{1}{1-\epsilon_p} \right) C_{smi} r^2 \, dr \right) \right], \quad i = 1,2,\ldots,n. \tag{24}$$

The term $\partial \bar{C}_{psi}/\partial t$ in Eqs. 1 and 1a is obtained [5,7] from

$$\frac{\partial \bar{C}_{psi}}{\partial t} = \frac{3}{2R_p^3}\left[\frac{\partial}{\partial t}\left(\int_0^{\pi}\int_0^{R_p} \epsilon_p C_{pi} R^2 \sin\theta \, dR \, d\theta \right) + \frac{\partial}{\partial t}\left(\int_0^{\pi}\int_0^{R_p} (1-\epsilon_p) \bar{C}_{si} R^2 \sin\theta \, dR \, d\theta \right) \right], \quad i = 1,2,\ldots,n, \tag{25}$$

where

$$\bar{C}_{si} = \frac{3}{r_m^3}\left[\int_0^{r_m} \epsilon_{pm} C_{pmi} r^2 \, dr + \int_0^{r_m} \left(\frac{1}{1-\epsilon_p}\right) C_{smi} r^2 \, dr\right], \quad i = 1,2,\ldots,n. \tag{26}$$

Finally, for a given pair of values of R and θ, the average concentration of component i in the adsorbed phase, $\bar{C}_{sai}$, is obtained [5,7] from the following expression:

$$\bar{C}_{sai} = (1-\epsilon_p)\frac{3}{r_m^3}\left[\int_0^{r_m} \left(\frac{1}{1-\epsilon_p}\right) C_{smi} r^2 \, dr\right], \quad i = 1,2,\ldots,m,m+1,\ldots,l. \tag{27}$$

For a given position x in the column, the average concentration of component i in the adsorbed phase, $C_{as,i}$, is given by

$$C_{as,i} = \frac{3}{2R_p^3}\int_0^{\pi}\int_0^{R_p} \bar{C}_{sai} R^2 \sin\theta \, dR \, d\theta, \quad i = 1,2,\ldots,m,m+1,\ldots,l. \tag{28}$$

The average concentration of component i in the adsorbed phase of the packed bed in the column of length L, is determined from the following expression:

$$\bar{C}_{as,i} = \frac{1}{L}\int_0^L C_{as,i} \, dx, \quad i = 1,2,\ldots,m,m+1,\ldots,l. \tag{29}$$

The dynamic behavior of a column adsorption system involving multi-component adsorption in spherical perfusive adsorbent particles with a bidisperse porous structure could be obtained by solving simultaneously Eqs. 1 (or 1a), 5 (or 5a), 16 (or 16a), and 17. If the intraparticle velocity is zero ($v_{pR} = v_{p\theta} = 0$), then the spherical adsorbent particles are considered to be purely diffusive. In this case, the concentration C_{pi} is considered to be independent of θ, and thus, the terms $\partial C_{pj}/\partial\theta$ ($j = 1,2,\ldots,n$) in Eq. 5 and $\partial C_{pi}/\partial\theta$ ($i = 1,2,\ldots,n$) in Eq. 5a are taken to be equal to zero; furthermore, the boundary conditions given by Eqs. 14 and 15 are not needed, and the boundary condition at $R = 0$ becomes $(\partial C_{pi}/\partial R)|_{R=0} = 0$ for $i = 1,2,\ldots,n$.

The solution of Eqs. 1a, 5a, 16a, and 17 for the binary adsorption system studied in this work, was obtained by adapting the numerical solution procedure reported in Ref. [5] to a system involving binary adsorption. It should be noted at this point that the numerical solution procedure reported in Ref. [5] could be adapted to obtain the solution of the equations of a multi-component adsorption system with $n \geq 2$.

The mathematical model that describes periodic counter-current adsorption is the same as that of a fixed-bed. The solution procedure for the single-column case can easily be adapted to the multi-column problem. After a column has been removed from the end of the sequence of columns corresponding to the fluid input and replaced by a fresh column at the other end, the initial conditions must be adjusted for the start of the new operating period. Those parts of the concentration profiles are deleted which correspond to the column that has been removed. The concentration profiles of the remaining columns are shifted, and the concentration profiles of the newly regenerated column are added at the other end.

The criterion for when to remove the bed at the upstream fluid end and to introduce a fresh bed at the other end can be based on the outlet concentration of the adsorbate(s).

3. Results and discussion

The mathematical model of multi-component perfusion chromatography presented in this work was used to study the dynamic behavior of a binary adsorption system. The expressions that describe the mass transfer step involving the dynamic adsorption mechanisms for components 1 and 2, for the system studied in this work, are as follows:

$$\frac{\partial C_{sm1}}{\partial t} = k_{11} C_{pm1}\left(C_{T1} - \sum_{j=1}^{2} C_{smj}\right) - k_{21} C_{sm1}, \tag{30}$$

$$\frac{\partial C_{sm2}}{\partial t} = k_{12} C_{pm2}\left(C_{T2} - \sum_{j=1}^{2} C_{smj}\right) - k_{22} C_{sm2}. \tag{31}$$

Table 1
Values of the fixed parameters of the binary perfusion chromatography system

Parameter	Value
$C_{d1,in}$	0.10 kg/m^3
C_{T1}	2.20 kg/m^3 particle
C_{T2}	2.20 kg/m^3 particle
D_{L1}	0
D_{L2}	0
d_m	7.0×10^{-7} m
D_{pm11}	3.74×10^{-12} m^2/s
D_{pm22}	9.69×10^{-12} m^2/s
k_{11}	0.235 m^3/kg · s
k_{12}	0.4108 m^3/kg · s
k_{21}	5.17×10^{-5} s^{-1}
k_{22}	2.222×10^{-2} s^{-1}
$K_{a,1} = k_{11}/k_{21}$	4545 m^3/kg
$K_{a,2} = k_{12}/k_{22}$	18.49 m^3/kg
L	0.1 m
T	296 K
ϵ	0.35
ϵ_{pm}	0.50

Eqs. 30 and 31 represent one possible functional form of the generalized form in Eq. 17. Parameter values of the binary perfusion chromatography system are listed in Tables 1 and 2. Table 1 lists the parameters that were not changed and Table 2 lists the parameters that were varied from case to case. The cases presented in Table 2 represent three different values for the macropore void fraction, ϵ_p, two different values for the particle diameter, d_p, and three different values for the inlet concentration of component 2, $C_{d2,in}$, examined in this work. For each case in Table 2, the superficial velocity, V_f, was varied over a range of values from 100–1000 cm/h, for both a single-column fixed-bed process and a two-column periodic counter-current process. For the cases with perfusive adsorbent particles, the value of F in Table 2 was calculated from Eq. 10 of Ref. [5] and, thus, the value of F is different for different values of ϵ_p and d_p. In the cases with $F = 0$, the adsorbent particles are considered to be purely diffusive. The values of D_{p11} and D_{p22} in Table 2 vary from case to case due to the dependence of the diffusivity upon ϵ_p. The values of C^*_{s1} and C^*_{s2} in Table 2 were obtained from the following equilibrium isotherm expressions, which are derived from Eqs. 30 and 31 by setting $\partial C_{sm1}/\partial t = \partial C_{sm2}/\partial t = 0$, $C_{pm1} = C_{d1,in}$ and $C_{pm2} = C_{d2,in}$:

$$C^*_{si} = \frac{C_{Ti} K_{a,i} C_{di,in}}{1 + \sum_{j=1}^{2} K_{a,j} C_{dj,in}}, \quad i = 1,2. \tag{32}$$

C^*_{s1} and C^*_{s2} are the equilibrium concentrations of species 1 and 2 in the adsorbed phase when the equilibrium concentrations of species 1 and 2 in the fluid phase are the inlet concentrations, $C_{d1,in}$ and $C_{d2,in}$. The values of the inlet concentration of species 1 and 2 in the flowing fluid stream remain constant for all times of the adsorption stage, indicating that the simulation studies of this work examine systems of frontal analysis.

For the binary system in this work, species 1 represents the most preferentially adsorbed component while species 2 is the least strongly adsorbed component. Component 1 is considered to be the

Table 2
Parameters of the binary perfusion chromatography system that were varied

	Case							
	1	2	3	4	5	6	7	8
ϵ_p	0.45	0.45	0.45	0.45	0.30	0.15	0.45	0.45
d_p (m)	1.5×10^{-5}	1.5×10^{-5}	1.5×10^{-5}	1.5×10^{-5}	1.5×10^{-5}	1.5×10^{-5}	3.0×10^{-5}	3.0×10^{-5}
F	7.236×10^{-3}	7.236×10^{-3}	7.236×10^{-3}	0	1.398×10^{-3}	1.218×10^{-3}	1.898×10^{-3}	0
$C_{d2,in}$ (kg/m^3)	0.10	0.01	0	0.10	0.10	0.10	0.10	0.10
C^*_{s1} (kg/m^3)	2.186	2.194	2.195	2.186	2.186	2.186	2.186	2.186
C^*_{s2} (kg/m^3)	8.892×10^{-3}	8.925×10^{-4}	0	8.892×10^{-3}	8.892×10^{-3}	8.892×10^{-3}	8.892×10^{-3}	8.892×10^{-3}
D_{p11} (m^2/s)	7.02×10^{-12}	7.02×10^{-12}	7.02×10^{-12}	7.02×10^{-12}	4.68×10^{-12}	2.34×10^{-12}	7.02×10^{-12}	7.02×10^{-12}
D_{p22} (m^2/s)	18.19×10^{-12}	18.19×10^{-12}	n/a	18.19×10^{-12}	12.13×10^{-12}	6.06×10^{-12}	18.19×10^{-12}	18.19×10^{-12}

n/a: not applicable.
Values of F are calculated from Eq. 10 of Ref. [5].

desired product and component 2 an undesired species (e.g., a contaminant). Therefore, increases in the concentration of component 1 and decreases in the concentration of component 2 in the adsorbed phase of a column to be regenerated are considered improvements in performance.

In the single-column fixed-bed system, the entire bed of adsorbent particles is regenerated when the concentration of component 1 in the exit stream is equal to 5% of the inlet concentration of component 1 ($C_{d1}(t,L) = 0.05C_{d1,in}$). In the two-column periodic counter-current system studied in this work, the column of length $L = 0.1$ m is divided into two columns each of length $L/2 = 0.05$ m and then these two columns are operated in periodic counter-current mode. The criterion used for when to switch columns under periodic counter-current operation is when the concentration of component 1 in the effluent is equal to 5% of the inlet concentration of component 1 ($C_{d1}(t,L) = 0.05C_{d1,in}$). The total length of the two-column periodic counter-current system is equal to the length of the single-column fixed-bed system. The first column of the periodic counter-current system is equivalent to the first half of the column of the fixed-bed system and the second column of the periodic counter-current system is equivalent to the second half of the column of the fixed-bed system.

In Figs. 1–3, the dimensionless concentration profiles of components 1 and 2 in the flowing fluid stream and in the adsorbed phase are presented for several times during the operation of a single fixed-bed at superficial velocities of 100, 500, and 1000 cm/h for the parameter values of case 1 of Table 2. The results for component 1 are represented by solid curves while those of component 2 are denoted by dashed curves. The last set of curves in each figure represents the concentration profiles at the end of an adsorption cycle, when 5% breakthrough of component 1 ($C_{d1}(t,L) = 0.05C_{d1,in}$) occurs.

The portion of the column in which adsorption of a species occurs is referred to in this work by the terms mass transfer zone, adsorption zone, and adsorption front, synonymously. For the binary system of this work, there will be two mass transfer zones, one for each of the two components. When flow to the column is initiated, the two adsorption fronts will coincide, but component 1, since it is most preferentially adsorbed, will propagate through

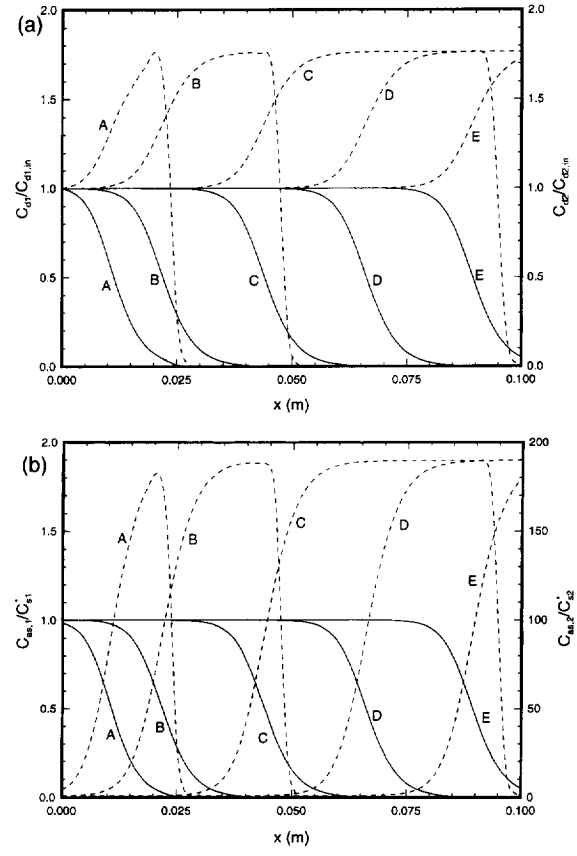

Fig. 1. Concentration profiles of component 1 and component 2 of the binary system (the solid curves are for component 1 and the dashed curves are for component 2) in the flowing fluid stream and in the adsorbed phase along the x-axis obtained from the single-column fixed-bed system with parameters of case 1 and $V_f = 100$ cm/h at different times. (A) 10 min; (B) 20 min; (C) 40 min; (D) 60 min; (E) 81 min. (a) $C_{d1}/C_{d1,in}$ and $C_{d2}/C_{d2,in}$ versus x; (b) $C_{as,1}/C^*_{s1}$ and $C_{as,2}/C^*_{s2}$ versus x.

the column slower than component 2. Thus the adsorption fronts of the two species will tend to separate. The results in Fig. 1a and b show that, at a superficial velocity of 100 cm/h, the mass transfer zones of the two species are completely separated by $t = 20$ min. When the adsorption zones of the two species are completely separated, component 2, in its mass transfer zone, will see a column free of component 1 and will adsorb to a concentration approaching its single-component equilibrium, which exceeds its binary equilibrium concentration. As the adsorption front of component 1 travels through the column, species 1 will adsorb and displace the

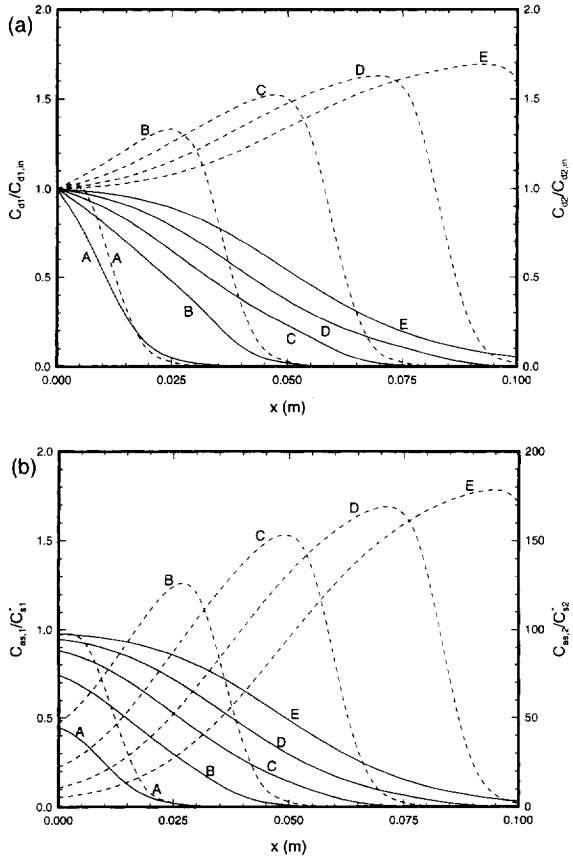

Fig. 2. Concentration profiles of component 1 and component 2 of the binary system (the solid curves are for component 1 and the dashed curves are for component 2) in the flowing fluid stream and in the adsorbed phase along the x-axis obtained from the single-column fixed-bed system with parameters of case 1 and $V_f = 500$ cm/h at different times. Curve: (A) 1 min; (B) 3 min; (C) 5 min; (D) 7 min; (E) 9.1 min. (a) $C_{d1}/C_{d1,in}$ and $C_{d2}/C_{d2,in}$ versus x; (b) $C_{as,1}/C^*_{s1}$ and $C_{as,2}/C^*_{s2}$ versus x.

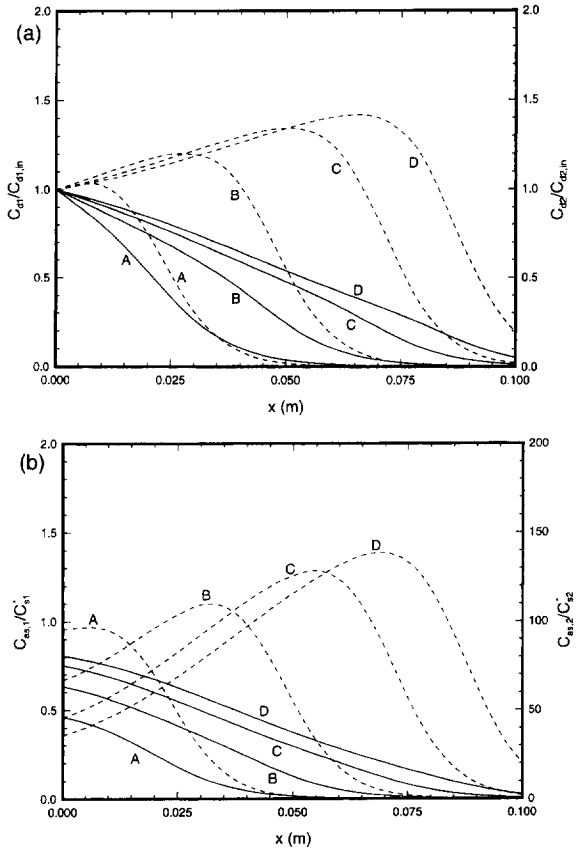

Fig. 3. Concentration profiles of component 1 and component 2 of the binary system (the solid curves are for component 1 and the dashed curves are for component 2) in the flowing fluid stream and in the adsorbed phase along the x-axis obtained from the single-column fixed-bed system with parameters of case 1 and $V_f = 1000$ cm/h at different times. Curve: (A) 1 min; (B) 2 min; (C) 3 min; (D) 3.65 min. (a) $C_{d1}/C_{d1,in}$ and $C_{d2}/C_{d2,in}$ versus x; (b) $C_{as,1}/C^*_{s1}$ and $C_{as,2}/C^*_{s2}$ versus x.

adsorbed species 2, which reenters the flowing fluid stream and increases the concentration of component 2 in the flowing fluid stream. This, in turn, further increases the adsorbed concentration of component 2 in its adsorption front. The net effect can be seen in the curves at $t = 40$ min in Fig. 1a and b. The concentrations of component 2 in the flowing fluid stream and in the adsorbed phase reach a peak between the two adsorption zones at values of about 1.8 and 190 times their respective equilibrium values. By $t = 81$ min, when 5% breakthrough of component 1 occurs, the mass transfer zone of component 2 and most of the concentration peak of component 2 have passed from the column.

The concentration profiles seen during the first cycle of periodic counter-current operation are the same as those shown in Fig. 1a and b for a single fixed bed. The curve at $t = 81$ min in Fig. 1b shows that the adsorbent in the first column, from $x = 0$ to 0.05 m, is completely saturated when the first column switch occurs. The adsorption zone of component 1 is entirely in the second column, from $x = 0.05$ to 0.1 m, when the column switch occurs, and therefore remains intact and is simply shifted to the first column during the column switch. In the

subsequent cycle, the adsorption front of component 1 propagates as before and a new adsorption front for component 2 forms ahead of the adsorption front of component 1.

The results in Fig. 2a and b indicate that when the superficial velocity is increased to 500 cm/h, the mass transfer zones of both species are lengthened, thus decreasing the degree of separation of the zones. The lengthened mass transfer zone of component 1 together with the decreased degree of separation of the adsorption fronts of the two species causes less of the component 2 concentration peak to exit the column before 5% breakthrough of component 1 occurs, compared to a superficial velocity of 100 cm/h. Thus the adsorbed concentration of component 1 is decreased and the adsorbed concentration of component 2 is increased, compared to a superficial velocity of 100 cm/h, for both fixed-bed operation and periodic counter-current operation.

When the superficial velocity is increased to 1000 cm/h, as the results in Fig. 3a and b show, the adsorption zones of the two species are lengthened and the degree of separation of the adsorption fronts is decreased to the point that the concentration peak of component 2 remains in the column when 5% breakthrough of component 1 occurs. When the column is operated in periodic counter-current mode, the concentration peak of component 2 is in the second column at the time of the first column switch, as shown by the curves at $t = 3.65$ min in Fig. 3a and b. Therefore the peak is retained in the column, and moved to the first column, during the switch. The amount of component 2 that enters the column during the subsequent cycle is greater than the amount that leaves the column in the exit stream and through the regeneration of the first column. Component 2 accumulates in the column from cycle to cycle, further lengthening the adsorption zones of the two species, until the amount leaving the column in the exit stream and through the regeneration of the first column balances that entering the column during a cycle.

In periodic counter-current operation, only the first column is regenerated when a column switch occurs, while in fixed-bed operation, the entire column is regenerated at the end of an adsorption cycle. Thus, the values of the bed average concentrations in the adsorbed phase, $\bar{C}_{as,1}$ and $\bar{C}_{as,2}$, as calculated from Eq. 29, that are reported in Table 3 and Figs. 4–6 are for the entire column at the time when 5% breakthrough of component 1 occurs in the fixed-bed system and just for the first column, at the end of a cycle after a number of cycles have passed that the system has reached periodic steady-state, in the two-column periodic counter-current system. In Figs. 4–6, the symbols represent simulation results; the symbols are connected by line segments.

In Fig. 4, the relationship between the dimensionless bed average concentration of component 1 in the adsorbed phase for a fixed-bed system and the superficial velocity in the column is shown for several values of the inlet concentration of component 2. Curves A, B, and C of Fig. 4 correspond with cases 1, 2, and 3 of Table 2, respectively. $\bar{C}_{as,1}/C^*_{s1}$ decreases as the superficial velocity is increased for all values of the inlet concentration of component 2, due to the lengthening of the adsorption fronts with increasing superficial velocity. When the inlet concentration of component 2 is zero or 0.01 kg/m^3, that is, much less than the inlet concentration of component 1, the decline in $\bar{C}_{as,1}/C^*_{s1}$ is nearly linear over the examined range of V_f. When the inlet concentration of component 2 is 0.10 kg/m^3, that is, equal to the inlet concentration of component 1, the decline in $\bar{C}_{as,1}/C^*_{s1}$ is greater than the decline in $\bar{C}_{as,1}/C^*_{s1}$ for lower concentrations of species 2, when V_f is less than 500 cm/h. But when the superficial velocity is increased above 500 cm/h, the rate of decline of the bed average adsorbed phase concentration of component 1 decreases to about the same rate of decline as for the lower inlet concentrations of component 2. When the superficial velocity is less than 500 cm/h, the adsorption zones of the two components are completely separated before 5% breakthrough of component 1 is reached. When V_f is greater than 500 cm/h, the two adsorption zones do not separate before 5% breakthrough of component 1 is reached. Thus, the concentration of component 2 in the adsorbed phase, which component 1 must displace in its adsorption front, is lower at superficial velocities above 500 cm/h than at superficial velocities less than 500 cm/h.

In Figs. 5 and 6, the results for the fixed-bed operating mode are represented by solid curves while those for the periodic counter-current operating mode

Table 3
Ratios of the bed average adsorbed phase concentration of component 1 to that of component 2 for fixed-bed and periodic counter-current systems

Case	V_t	$Pe_{intra.1}$	$Pe_{intra.2}$	$\bar{C}_{as,1}/\bar{C}_{as,2}$	
	(cm/h)			Fixed-bed system	Periodic counter-current system
1	100	4.3	1.7	10.7	246
	300	12.9	5.0	2.93	52.6
	500	21.5	8.3	1.31	4.79
	750	32.2	12.4	1.13	1.25
	1000	43.0	16.6	1.10	1.13
2	100	4.3	1.7	32.6	2459
	300	12.9	5.0	12.9	2459
	500	21.5	8.3	11.6	511
	750	32.2	12.4	11.3	51.8
	1000	43.0	16.6	11.1	20.8
3	100	4.3	n/a	n/a	n/a
	300	12.9	n/a	n/a	n/a
	500	21.5	n/a	n/a	n/a
	750	32.3	n/a	n/a	n/a
	1000	43.0	n/a	n/a	n/a
4	100	0	0	10.7	246
	300	0	0	2.80	47.4
	500	0	0	1.26	4.22
	750	0	0	1.13	1.25
	1000	0	0	1.09	1.11
5	100	1.2	0.5	9.48	246
	300	3.7	1.4	2.40	29.6
	500	6.2	2.4	1.19	2.77
	750	9.3	3.6	1.11	1.15
	1000	12.4	4.8	1.08	1.09
6	100	2.2	0.8	6.05	246
	300	6.5	2.5	1.29	4.56
	500	10.8	4.2	1.11	1.18
	750	16.3	6.3	1.04	1.04
	1000	21.7	8.4	0.979	0.985
7	100	2.2	0.9	8.38	246
	300	6.8	2.6	1.99	17.0
	500	11.3	4.3	1.17	1.84
	750	16.9	6.5	1.10	1.15
	1000	22.5	8.7	1.07	1.07
8	100	0	0	8.38	246
	300	0	0	1.94	15.5
	500	0	0	1.16	1.59
	750	0	0	1.09	1.12
	1000	0	0	1.05	1.04

n/a: not applicable.

are represented by dashed curves. Fig. 5a and b show the relationship between the dimensionless bed average adsorbed phase concentration of components 1 and 2, respectively, and the superficial velocity in the column for different values of ϵ_p for both fixed-bed operation and periodic counter-current operation. Curves A, B, and C of Fig. 5a and b correspond with cases 1, 5, and 6 of Table 2, respectively. Fig. 5a shows that $\bar{C}_{as,1}/C^*_{s1}$ decreases as ϵ_p is decreased. The mass transfer resistance within the macroporous region of the adsorption particle increases as ϵ_p decreases and increased mass transfer resistance lengthens the adsorption fronts, thus reducing the bed average concentration of component 1 in the

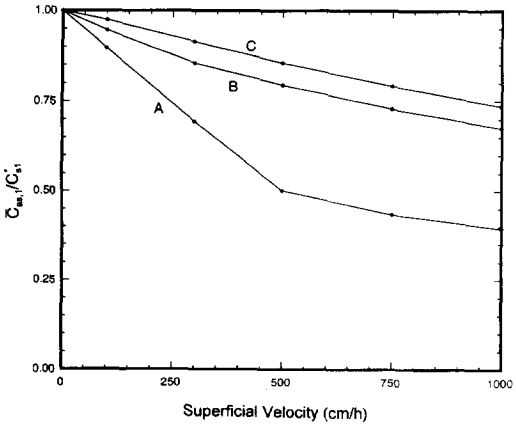

Fig. 4. Bed average concentration of component 1 in the adsorbed phase versus superficial velocity obtained from the single-column fixed-bed system for different values of the inlet concentration of component 2, $C_{d2,in}$. Curve: (A) case 1, $C_{d2,in} = 0.10$ kg/m^3; (B) case 2, $C_{d2,in} = 0.01$ kg/m^3; (C) case 3, $C_{d2,in} = 0$.

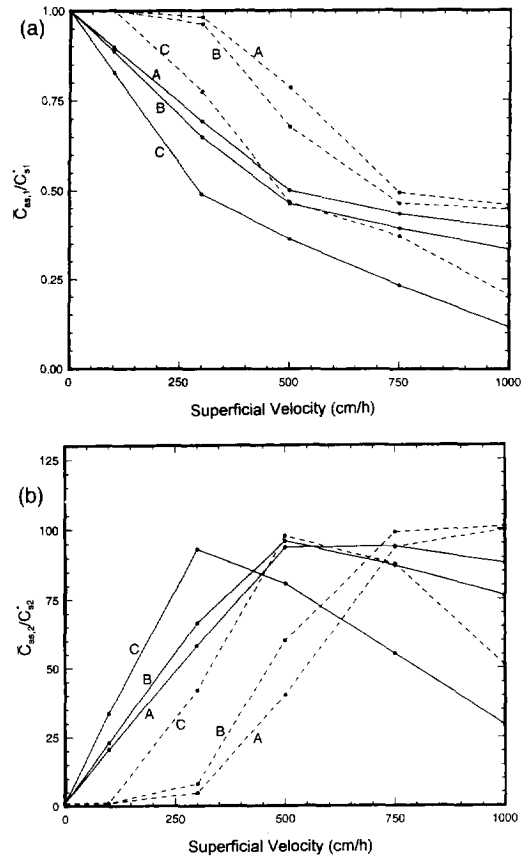

Fig. 5. Bed average concentrations of components 1 and 2 in the adsorbed phase versus superficial velocity obtained from the single-column fixed-bed and two-column periodic counter-current systems (the solid curves are for the fixed-bed system and the dashed curves are for the periodic counter-current system) for different values of the macropore void fraction, ϵ_p. Curve: (A) case 1, $\epsilon_p = 0.45$; (B) case 5, $\epsilon_p = 0.30$; (C) case 6, $\epsilon_p = 0.15$. (a) $\bar{C}_{as,1}/C^*_{s1}$ versus V_f; (b) $\bar{C}_{as,2}/C^*_{s2}$ versus V_f.

adsorbed phase. In Fig. 5b, for each ϵ_p in the fixed-bed operating mode, $\bar{C}_{as,2}/C^*_{s2}$ increases with increasing superficial velocity to a peak, then declines as the superficial velocity is further increased. When the value of the superficial velocity is low, an increase in the superficial velocity causes less of the concentration peak of component 2 to exit the column before component 1 breaks through, thereby increasing the bed average adsorbed phase concentration of component 2. When the superficial velocity is high enough that the component 2 concentration peak remains within the column when component 1 breaks through, an increase in V_f causes less component 2 to be adsorbed before component 1 breaks through, thereby decreasing the bed average adsorbed phase concentration of component 2. The superficial velocity at which the value of $\bar{C}_{as,2}/C^*_{s2}$ peaks is lower at smaller ϵ_p, due to the lengthened adsorption fronts caused by increased mass transfer resistance.

The value of $\bar{C}_{as,1}/C^*_{s1}$ in Fig. 5a for a periodic counter-current system is higher than that for a fixed-bed system for each ϵ_p at all superficial velocities. The value of $\bar{C}_{as,2}/C^*_{s2}$ in Fig. 5b is lower for a periodic counter-current system than for a fixed-bed system for each ϵ_p at low superficial velocities. But at higher superficial velocities, the value of $\bar{C}_{as,2}/C^*_{s2}$ is higher for periodic counter-current operation than for fixed-bed operation, due to the cycle-to-cycle accumulation of component 2 in periodic counter-current operation.

Fig. 6a and b show the relationship between the dimensionless bed average adsorbed phase concentration of components 1 and 2, respectively, and the superficial velocity in the column, for perfusive particles and purely diffusive particles at two values of d_p for both fixed-bed operation and periodic counter-current operation. Curves A, B, C, and D of Fig. 6 correspond with cases 1, 4, 7, and 8 of Table 2. The results in Fig. 6a and b indicate that the

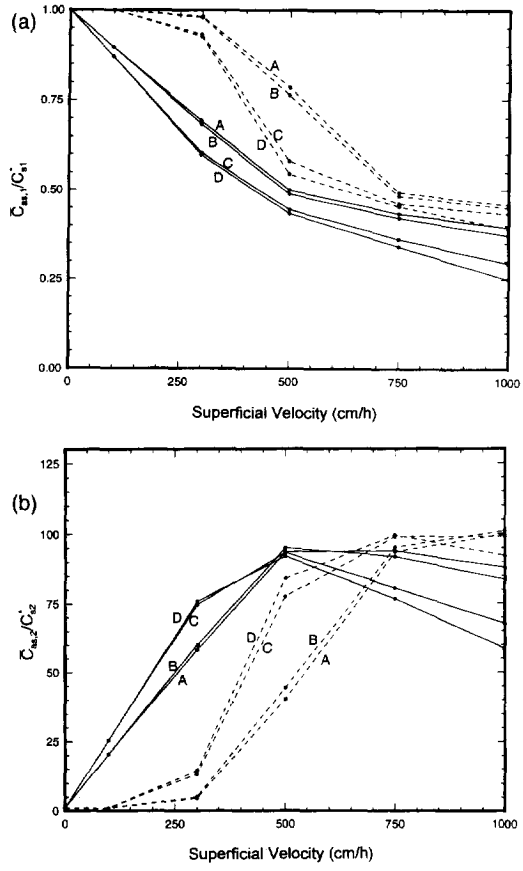

Fig. 6. Bed average concentrations of components 1 and 2 in the adsorbed phase versus superficial velocity obtained from the single-column fixed-bed and two-column periodic counter-current systems (the solid curves are for the fixed-bed system and the dashed curves are for the periodic counter-current system) for perfusive and purely diffusive adsorbent particles for different values of the particle diameter, d_p. Curve: (A) case 1, $d_p = 1.5 \times 10^{-5}$ m, $F = 7.236 \times 10^{-3}$; (B) case 4, $d_p = 1.5 \times 10^{-5}$ m, $F = 0$; (C) case 7, $d_p = 3.0 \times 10^{-5}$ m, $F = 1.898 \times 10^{-3}$; (D) case 8, $d_p = 3.0 \times 10^{-5}$ m, $F = 0$. (a) $\bar{C}_{as,1}/C^*_{s1}$ versus V_f; (b) $\bar{C}_{as,2}/C^*_{s2}$ versus V_f.

performance of particles with $d_p = 1.5 \times 10^{-5}$ m is better than the performance of particles with $d_p = 3.0 \times 10^{-5}$ m for both fixed-bed and periodic counter-current systems, due to greater mass transfer resistance in the larger particles. For both particle diameters, the values of $\bar{C}_{as,1}/C^*_{s1}$ and $\bar{C}_{as,2}/C^*_{s2}$ are the same for perfusive particles and purely diffusive particles when the superficial velocity is low and become only slightly different as V_f is increased. The intraparticle Péclet numbers of components 1 and 2 for each case at every value of V_f considered in this work are presented in Table 3. For cases 1 and 7, the cases in Fig. 6 with perfusive particles, both $Pe_{intra,1}$ and $Pe_{intra,2}$ are less than 5 at $V_f = 100$ cm/h. Thus, the fact that there is no difference between the performance of perfusive particles and the performance of purely diffusive particles at that superficial velocity agrees with the results for single-component adsorption [5,7], where it was shown that the intraparticle Péclet number had to be greater than 10 for there to be a clear difference between the performance of perfusive particles and the performance of purely diffusive particles.

In Figs. 7 and 8, the dimensionless isoconcentration profiles of component 1 and component 2, respectively, in the pore fluid of the pores of the macroporous region of the adsorbent particle are presented, while in Figs. 9 and 10, the dimensionless isoconcentration profiles of component 1 and component 2, respectively, in the adsorbed phase of the adsorbent particle are shown, at position $x = 0.25L = 0.025$ m of the single fixed-bed and at three times: $t = 1.0$, 1.5, and 2.0 min. In Figs. 7–10, the outermost contours represent the isoconcentrations at the surface ($R = R_p$) of the particle.

The data in Figs. 7–10 have been obtained with a superficial velocity of 1000 cm/h and the parameter values of case 1 of Table 2; from Table 3 it is observed that the values of $Pe_{intra,1}$ and $Pe_{intra,2}$ are 43.0 and 16.6, respectively. The isoconcentration profiles in Figs. 7–10 exhibit spherical asymmetry, as expected for adsorption in perfusive particles. It should be noted at this point that the isoconcentration profiles of components 1 and 2 in the pore fluid of the pores of the macroporous region and in the adsorbed phase of a purely diffusive particle represented by case 4 ($Pe_{intra,1} = Pe_{intra,2} = 0$) of Table 2 and obtained with a superficial velocity of 1000 cm/h, exhibit spherical symmetry [30], as expected for adsorption in purely diffusive particles.

The isoconcentration profiles of the most preferentially adsorbed component 1, as shown in Figs. 7 and 9, have a shape similar to isoconcentration profiles of adsorbate in single-component adsorption at a similar value of the intraparticle Péclet number [5,7]. The shape of the isoconcentration contours of component 1 does not change with time, although the values of the concentrations are increasing;

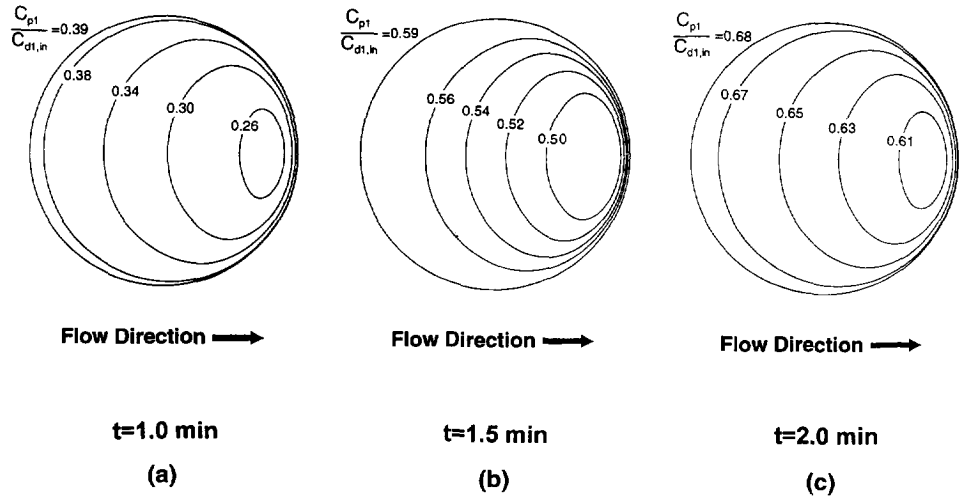

Fig. 7. Isoconcentration contours of the concentration of component 1 in the pore fluid of the macroporous region of the porous adsorbent particle for case 1 with V_f = 1000 cm/h, at $x = 0.25L$ for different times. (a) t = 1 min; (b) t = 1.5 min; (c) t = 2 min.

furthermore, the results in Figs. 7 and 9 clearly indicate that the values of the concentrations of the outermost contours are higher than the values of the concentrations of all internal contours at all times.

The isoconcentration profiles of the less preferentially adsorbed component 2 in the macropore fluid, as shown in Fig. 8, have a different shape than the isoconcentration profiles of component 1. The isoconcentration profiles of component 2 in the adsorbed phase, as shown in Fig. 10, have a different shape than the isoconcentration profiles of component 1 for t = 1.0 and 1.5 min, while for t = 2.0 min the shape of the isoconcentration profiles of components 1 and 2 in the adsorbed phase, as shown in Figs. 9 and 10, is similar. Furthermore, the results in Figs. 8 and 10 indicate that for certain times, the values of the concentrations of the outermost contours are lower than the values of the concentrations of the internal isoconcentration contours. It should be noted that when the adsorption process starts, com-

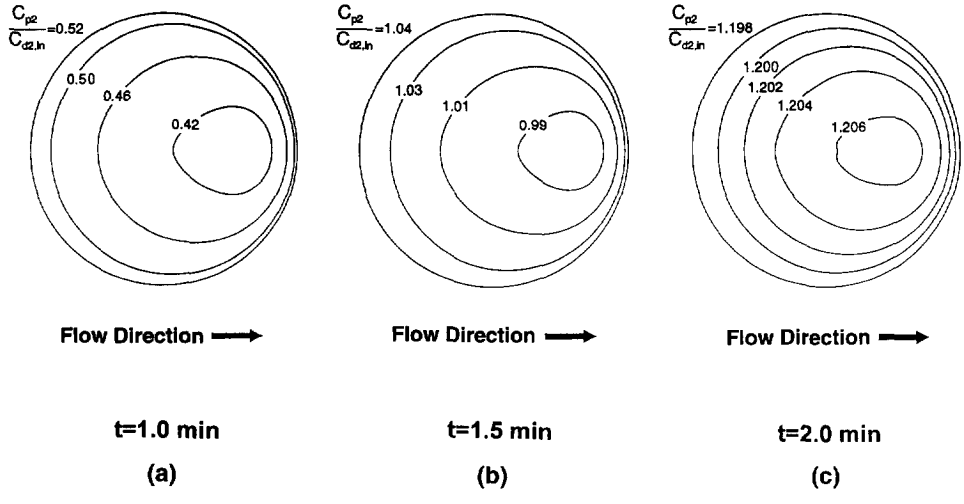

Fig. 8. Isoconcentration contours of the concentration of component 2 in the pore fluid of the macroporous region of the porous adsorbent particle for case 1 with V_f = 1000 cm/h, at $x = 0.25L$ for different times. (a) t = 1 min; (b) t = 1.5 min; (c) t = 2 min.

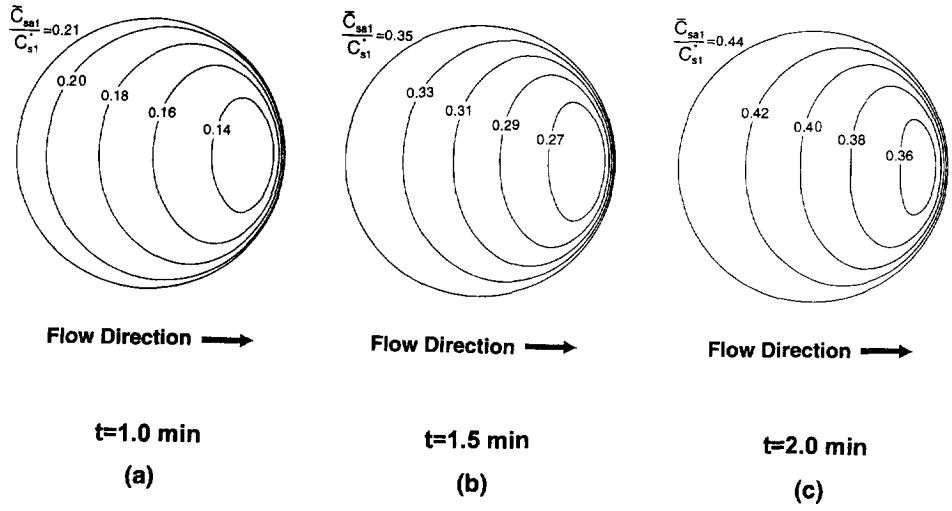

Fig. 9. Isoconcentration contours of the concentration of component 1 in the adsorbed phase of the porous adsorbent particle for case 1 with V_f = 1000 cm/h, at $x = 0.25L$ for different times. (a) t = 1 min; (b) t = 1.5 min; (c) t = 2 min.

ponents 1 and 2 move from the surface of the particle by intraparticle convective flow and diffusion; but, the diffusion coefficient of the less preferentially adsorbed component 2 is about 2.59 times larger than the diffusion coefficient of the most preferentially adsorbed component 1. Thus, depending, for a given value of t, on (i) the distribution of the penetration lengths of components 1 and 2 in the particle, (ii) the values of the local rates of adsorption of components 1 and 2 at different positions along each of the penetration lengths, and (iii) the values of the local rate of displacement of component 2 by component 1 at different positions along each of the penetration lengths, isoconcentration contours could be obtained with geometries and distribution of concentration values at different parts of the particle as those shown in Figs. 8 and 10 for the less preferentially adsorbed component 2.

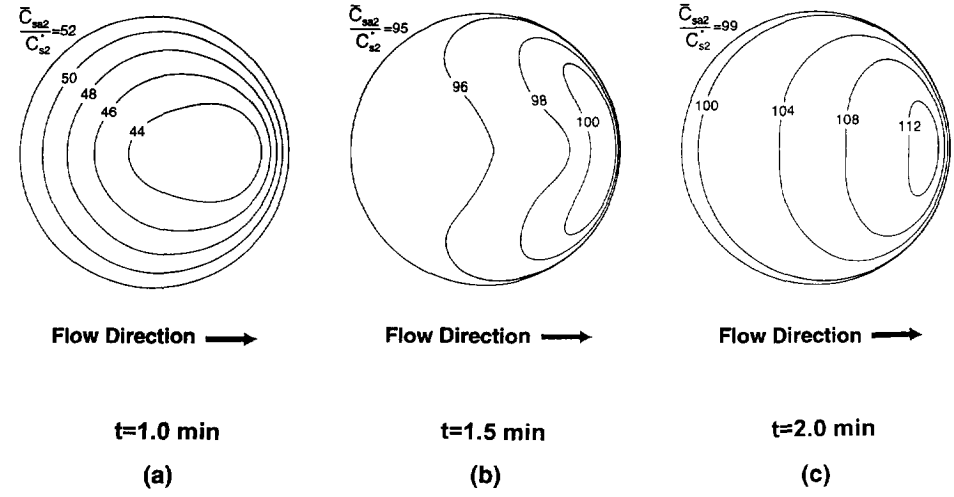

Fig. 10. Isoconcentration contours of the concentration of component 2 in the adsorbed phase of the porous adsorbent particle for case 1 with V_f = 1000 cm/h, at $x = 0.25L$ for different times. (a) t = 1 min; (b) t = 1.5 min; (c) t = 2 min.

The ratio of the bed average concentration of component 1 in the adsorbed phase to the bed average concentration of component 2 in the adsorbed phase for each case at every superficial velocity considered in this work for both the fixed-bed and the periodic counter-current operation mode is presented in Table 3. For every case, the ratio $\bar{C}_{as,1}/\bar{C}_{as,2}$ decreases as V_f is increased in both fixed-bed and periodic counter-current systems. Also, comparing cases 1, 5, and 6, which differ only by the value of ϵ_p, shows that, at each value of V_f, $\bar{C}_{as,1}/\bar{C}_{as,2}$ decreases as ϵ_p is decreased. Comparing cases 1 and 7, which differ only by the value of d_p, shows that, at each value of V_f, $\bar{C}_{as,1}/\bar{C}_{as,2}$ decreases as d_p is increased. Thus, any change that lengthens the adsorption zones of the two species, whether increasing the superficial velocity, V_f, or increasing the mass transfer resistance by decreasing ϵ_p or increasing d_p, will cause the ratio $\bar{C}_{as,1}/\bar{C}_{as,2}$ to decrease. Comparing cases 1 and 4 and cases 7 and 8, which differ only in that the first case of each pair has perfusive adsorbent particles and the second case of each pair has purely diffusive adsorbent particles, shows that there is little or no difference between the ratio $\bar{C}_{as,1}/\bar{C}_{as,2}$ for perfusive particles and that for purely diffusive particles at any superficial velocity in either the fixed-bed operating mode or the periodic counter-current operating mode. The intraparticle fluid flow in the perfusive particles does not significantly reduce the overall mass transfer resistance because the rates of the interaction of the two adsorbates with the solid surface are not infinitely fast and the finite rates of the adsorption mechanisms contribute significantly to the overall mass transfer resistance within the particles.

When the superficial velocity is low, the ratio $\bar{C}_{as,1}/\bar{C}_{as,2}$ in the periodic counter-current operating mode is much higher than that in the fixed-bed operating mode for every case. But, as V_f is increased, the difference between $\bar{C}_{as,1}/\bar{C}_{as,2}$ for fixed-bed and periodic counter-current systems decreases, until, at a superficial velocity of 1000 cm/h, operating in the periodic counter-current mode does not produce a clear improvement in the ratio $\bar{C}_{as,1}/\bar{C}_{as,2}$ over operating in the fixed-bed mode. In fact, at a superficial velocity of 1000 cm/h, the value of $\bar{C}_{as,1}/\bar{C}_{as,2}$ for periodic counter-current and fixed-bed systems for every case is not much larger than the ratio of the concentration of component 1 to that of component 2 in the inlet stream (in one case, case 6, the ratio $\bar{C}_{as,1}/\bar{C}_{as,2}$ is even less than the ratio of $C_{d1,in}$ to $C_{d2,in}$). Therefore, the ratio of the amount of the desired species to the amount of the undesired species in the product stream obtained in the elution stage would be little better than that in the feed stream during the adsorption stage, indicating that the separation efficiency of the process is rather poor. On the other hand, at a superficial velocity of 100 cm/h, $\bar{C}_{as,1}/\bar{C}_{as,2}$ for a periodic counter-current system is its maximum possible value for every case. The maximum possible value of $\bar{C}_{as,1}/\bar{C}_{as,2}$ is reached when the concentrations in the adsorbed phase are at equilibrium with the inlet concentrations. The separation that can be achieved in the periodic counter-current system operating at a superficial velocity of 100 cm/h depends upon the equilibrium isotherms but does not depend upon the values of ϵ_p or d_p or whether the adsorbent particles are perfusive or purely diffusive, because the column to be regenerated is at equilibrium with the feed composition.

4. Conclusions and remarks

A mathematical model of multi-component adsorption in columns packed with spherical perfusive and spherical purely diffusive adsorbent particles with a bidisperse porous structure was presented and used to study the dynamic behavior of a binary adsorption system in a single-column fixed-bed process and in a two-column periodic counter-current process. The performance of chromatographic columns, as measured by the concentrations of the two species in the adsorbed phase of a column being regenerated, was compared for both single-column fixed-bed and two-column periodic counter-current systems for both perfusive and purely diffusive adsorbent particles for different values of the macropore void fraction, ϵ_p, the particle diameter, d_p, the inlet concentration of the least preferentially adsorbed component 2, $C_{d2,in}$, and the superficial velocity, V_f.

The performance that is achieved by a chromato-

graphic system depends upon the length of the adsorption zones of the two species and the degree of separation of those zones at the time the most preferentially adsorbed component 1 breaks through. When the system parameters are such that the two mass transfer zones are short and completely separated at breakthrough, then the ratio of the bed average concentration of component 1 in the adsorbed phase to that of component 2 can be many times greater than the ratio of the concentration of component 1 to that of component 2 in the feed, and the relative separation efficiency is high. When the system parameters are changed such that the adsorption fronts are lengthened and overlap, the performance can deteriorate until the ratio of the bed average adsorbed phase concentration of component 1 to that of the component 2 is no better than the ratio of the concentration of component 1 to that of component 2 in the feed and no separation is taking place. Either increasing the superficial velocity, V_f, or increasing the mass transfer resistance by decreasing ϵ_p or increasing d_p will lengthen the adsorption zones and thus result in poorer performance. However, the performance of systems with perfusive adsorbent particles is only slightly better than the performance of systems with purely diffusive adsorbent particles, because the intraparticle fluid flow in the perfusive particles does not significantly reduce the overall mass transfer resistance because the finite rates of the adsorption mechanisms contribute significantly to the overall mass transfer resistance within the particles.

The isoconcentration profiles of the most preferentially adsorbed component 1 inside a perfusive adsorbent particle exhibit the same asymmetric shape as the isoconcentration profiles of adsorbate in single-component adsorption. However, the isoconcentration profiles of the least preferentially adsorbed component 2 can, for certain times, have distinctly different shapes. The shape of the isoconcentration contours of component 2 depends upon the distribution of the penetration lengths of components 1 and 2 in the particle and the values of the local rates of adsorption of components 1 and 2 and of the displacement of component 2 by component 1 at different positions along each of the penetration lengths.

At low superficial velocity, V_f, the performance of the two-column periodic counter-current system is much better than the performance of the single-column fixed-bed system, but the advantage of periodic counter-current operation over fixed-bed operation disappears as V_f is increased. For all cases considered in this work, the best possible performance is achieved in the periodic counter-current operating mode at a superficial velocity of 100 cm/h. Changes in the values of ϵ_p and d_p of the adsorbent particle have no effect on the performance of systems operating in the periodic counter-current mode, as long as the superficial velocity is low enough that the adsorption front of component 1 is entirely within the second column at the time at which column switch occurs. Increasing the overall length of the column could allow the superficial velocity to be increased yet keep the adsorption front of component 1 entirely within the second column at the time at which column switch occurs, thus maintaining high relative separation efficiency. Dividing the column into more than two beds for periodic counter-current operation could also allow the superficial velocity, V_f, to be increased and still maintain high relative separation efficiency. The product purity is determined by the ratio of the desired component 1 to the unwanted component 2 in the adsorbed phase of the column to be regenerated. If a higher purity is required, it could be achieved by using a multi-column adsorption–elution system in which the effluent obtained from a periodic counter-current adsorption bed during the elution stage becomes the feed to another periodic counter-current adsorption column system during the adsorption stage; this mode of operation could multiply the chromatographic effect of the relative separation between species 1 and 2.

5. Symbols

$C_{as,i}$	average concentration of component i in the adsorbed phase defined in Eq. 28 (kg/m^3 of adsorbent particle),
$\bar{C}_{as,i}$	bed average concentration of component i in the adsorbed phase defined in Eq. 29 (kg/m^3 of adsorbent particle),

C_{di} concentration of component i in the flowing fluid stream of the column (kg/m^3 of bulk fluid),

$C_{di,in}$ concentration of component i at $x<0$ when $D_{Li}\neq 0$, or at $x=0$ when $D_{Li}=0$ (kg/m^3 of bulk fluid),

C_{pi} concentration of component i in the fluid of the macropores (throughpores) (kg/m^3 of macropore volume),

$\mathbf{C}_{pm}$ vector of the concentrations of the adsorbates in the micropore fluid, defined after Eq. 17,

C_{pmi} concentration of component i in the fluid of the micropores (kg/m^3 of micropore volume),

$\bar{C}_{psi}$ average concentration of component i in the adsorbent particle (kg/m^3 of adsorbent particle),

$\bar{C}_{sai}$ average concentration of component i in the adsorbed phase defined in Eq. 27 (kg/m^3 of adsorbent particle),

$\bar{C}_{si}$ average concentration of component i defined in Eq. 26 (kg/m^3 of microparticle),

C^*_{si} equilibrium concentration of component i in the adsorbed phase given by Eq. 32 (kg/m^3 of adsorbent particle),

$\mathbf{C}_{sm}$ vector of the concentrations of the adsorbates in the adsorbed phase, defined after Eq. 17,

C_{smi} concentration of component i in the adsorbed phase of the microparticle (kg/m^3 of adsorbent particle),

C_{Ti} maximum equilibrium concentration of component i in the adsorbed phase of the microparticle (kg/m^3 of adsorbent particle),

d_m diameter of spherical microparticle ($d_m=2r_m$) (m),

d_p diameter of spherical porous adsorbent particle ($d_p=2R_p$) (m),

D_{Li} axial dispersion coefficient of component i (m^2/s),

$\mathbf{D}_p$ effective pore diffusivity matrix in the macropores,

D_{pij} effective pore diffusion coefficients in the macropores (elements of the effective pore diffusivity matrix $\mathbf{D}_p$ in the macropores) (m^2/s),

$\mathbf{D}_{pm}$ effective pore diffusivity matrix in the micropores,

D_{pmij} effective pore diffusion coefficients in the micropores (elements of the effective pore diffusivity matrix $\mathbf{D}_{pm}$ in the micropores) (m^2/s),

$\mathbf{D}_{sm}$ surface diffusivity matrix in the microspheres (microparticles),

D_{smij} surface diffusion coefficients in the microspheres (microparticles) (elements of the surface diffusivity matrix $\mathbf{D}_{sm}$ in the microspheres (microparticles)) (m^2/s),

$f_i(\mathbf{C}_{pm},\mathbf{C}_{sm},\mathbf{k})$ functional form defined after Eq. 17,

F parameter given by Eq. 10 of Ref. [5],

$g_i(\mathbf{C}_{pm},\mathbf{K})$ functional form defined after Eq. 19,

H parameter given by Eq. 11 of Ref. [5],

$\mathbf{k}$ vector of adsorption rate constants defined after Eq. 17,

k_{11} adsorption rate constant for component 1 in Eq. 30 (m^3 of micropore volume/kg·s),

k_{12} adsorption rate constant for component 2 in Eq. 31 (m^3 of micropore volume/kg·s),

k_{21} adsorption rate constant for component 1 in Eq. 30 (s^{-1}),

k_{22} adsorption rate constant for component 2 in Eq. 31 (s^{-1}),

$\mathbf{K}$ vector of the equilibrium adsorption constants defined after Eq. 19,

$K_{a,i}$ equilibrium adsorption constant of component i, $K_{a,i}=k_{1i}/k_{2i}$ (m^3 of micropore volume/kg),

l total number of components adsorbed by specific and non-specific adsorption,

L column length (m),

m total number of components adsorbed by specific adsorption,

n total number of components,

$Pe_{intra,i}$ intraparticle Péclet number of component i defined in Eq. 9 (dimensionless),
r radial distance in microparticle (m),
r_m radius of microparticle (m),
R radial distance in adsorbent particle (m),
R_p radius of adsorbent particle (m),
t time (s),
T temperature (K),
$\boldsymbol{v}_p$ intraparticle velocity vector (m/s),
v_{pR} intraparticle velocity component along the R direction (m/s),
v_{px_1} axial component of the intraparticle velocity given by Eq. 18 of Ref. [5] (m/s),
$v_{p\theta}$ intraparticle velocity component along the θ direction (m/s),
V_f column fluid superficial velocity (m/s),
x axial distance in column (m),
x_1 axial coordinate of adsorbent particle as shown in Fig. 1 of Ref. [5] (m).

5.1. Greek letters

ϵ void fraction in column,
ϵ_p macropore (through-pore) void fraction,
ϵ_{pm} micropore void fraction,
θ polar coordinate angle (rad).

Acknowledgments

The authors gratefully acknowledge partial support of this work by Monsanto.

References

[1] A.I. Liapis and M.A. McCoy, J. Chromatogr., 599 (1992) 87.
[2] M.A. McCoy, A.I. Liapis and K.K. Unger, J. Chromatogr., 644 (1993) 1.
[3] A.I. Liapis, Math. Model. Sci. Comput., 1 (1993) 397.
[4] A.I. Liapis and M.A. McCoy, J. Chromatogr. A, 660 (1994) 85.
[5] A.I. Liapis, Y. Xu, O.K. Crosser and A. Tongta, J. Chromatogr. A, 702 (1995) 45.
[6] A.I. Liapis and K.K. Unger, in G. Street (Editor), Highly Selective Separations in Biotechnology, Blackie Academic and Professional, An imprint of Chapman and Hall, Glasgow, 1994, pp. 121–162.
[7] G.A. Heeter and A.I. Liapis, J. Chromatogr. A, 711 (1995) 3.
[8] Y. Xu and A.I. Liapis, J. Chromatogr. A, 724 (1996) 13.
[9] N.B. Afeyan, N.F. Gordon, I. Mazsaroff, L. Varady, S.P. Fulton, Y.B. Yang and F.E. Regnier, J. Chromatogr., 519 (1990) 1.
[10] N.B. Afeyan, S.P. Fulton, N.F. Gordon, I. Mazsaroff, L. Varady and F.E. Regnier, Biotechnology, 8 (1990) 203.
[11] B.H. Arve and A.I. Liapis, Biotechnol. Bioeng., 32 (1988) 616.
[12] A.I. Liapis, Sep. Purif. Methods, 19 (1990) 133.
[13] F.H. Arnold, H.W. Blanch and C.R. Wilke, Chem. Eng. J., 30 (1985) B9.
[14] B.H. Arve and A.I. Liapis, AIChE J., 33 (1987) 179.
[15] J.H. Harwell, A.I. Liapis, R.J. Litchfield and D.T. Hanson, Chem. Eng. Sci., 35 (1980) 2287.
[16] C.J. Geankoplis, Transport Processes and Unit Operations, Allyn and Bacon, Boston, 2nd ed., 1983.
[17] G. Neale, N. Epstein and W. Nader, Chem. Eng. Sci., 28 (1973) 1865.
[18] F.H. Arnold, H.W. Blanch and C.R. Wilke, Chem. Eng. J., 30 (1985) B25.
[19] D.J. Gunn, Trans. Inst. Chem. Eng., 49 (1971) 109.
[20] D.J. Gunn, Chem. Eng. Sci., 42 (1987) 363.
[21] H.L. Toor and K.R. Arnold, Ind. Eng. Chem. Fundam., 4 (1965) 363.
[22] A.I. Liapis and R.J. Litchfield, Trans. Inst. Chem. Eng., 59 (1981) 122.
[23] G. Stephanopoulos and K. Tsiveriotis, Chem. Eng. Sci., 44 (1989) 2031.
[24] M.A. McCoy and A.I. Liapis, J. Chromatogr., 548 (1991) 25.
[25] D.M. Ruthven, Principles of Adsorption and Adsorption Processes, Wiley, New York, 1984.
[26] R.L. Beissinger and E.F. Leonard, J. Colloid Interface Sci., 85 (1982) 521.
[27] G. Guiochon, S.G. Shirazi and A.M. Katti, Fundamentals of Preparative and Nonlinear Chromatography, Academic Press, New York, 1994.
[28] J.H. Petropoulos, J.K. Petrou and A.I. Liapis, Ind. Eng. Chem. Res., 30 (1991) 1281.
[29] J.H. Petropoulos, A.I. Liapis, N.P. Kolliopoulos, J.K. Petrou and N.K. Kanellopoulos, Bioseparation, 1 (1990) 69.
[30] G.A. Heeter, Internal Report, Department of Chemical Engineering, University of Missouri-Rolla, Rolla, MO, 1995.